AN INVESTIGATION OF HIGH VELOCITY RADIAL AIR FLOW

by

Mark M. Gantar, Lt. Comdr., USN

R.P.I., Troy, N. Y. May 1948

AN INVESTIGATION OF HIGH VELOCITY RADIAL AIR FLOW

by

Mark M. Gantar
Lieutenant Commander
United States Navy

Submitted in partial fulfillment of the requirements for the degree of Master of Science at Rensselaer Polytechnic Institute.

May 1948

ACKNOWLEDGMENT

The writer wishes to express his deep appreciation to Professor Neil P. Bailey for his assistance and guidance in this investigation, and for the cooperation of Professor James J. Devine, and the exacting machine work of W. E. Goyer.

TABLE OF CONTENTS

Figures	Figure No.

AN INVESTIGATION OF HIGH VELOCITY RADIAL AIR FLOW

SUMMARY

The investigation of high velocity air flow in a radial, parallel-walled passage was conducted to determine; first, whether or not a diverging physical boundary is necessary to produce super-acoustic acceleration, and second, if supersonic velocities can be attained what type of discontinuity, if any, occurs.

A limit of the investigation was the amount of air available. Available air dictated such small flow areas that boundary layer conditions materially affected net flow area. Therefore, all conclusions of this investigation apply to air flow in a parallel-walled, radial passage with very small flow area such that flow dimensions are the same order of magnitude as boundary layer thickness.

It was found that a positive area gradient without a diverging boundary was a sufficient condition to produce super-acoustic acceleration. It was also found that no discontinuities exist in the passage; and that friction factors, when corrected for probable boundary layer, can be considered constant. Finally, a radial parallel-walled passage, with flow clearance the same order of

magnitude as boundary layer thickness, can be used to conduct fundamental supersonic flow studies where discontinuities are undesirable.

AN INVESTIGATION OF HIGH VELOCITY RADIAL AIR FLOW

INTRODUCTION

The study of air flow at high velocities has been extensively carried out in constant area, converging, and diverging passages. In addition, the birth of the supersonic age has given a great impetus to this study. However, no records can be found of any previous investigation of high velocity air flow in a radial passage.

This investigation was conducted with a radial passage designed with converging walls approaching a minimum area throat section followed by parallel walls as shown in Figure 1. The study of high velocity air flow under these conditions presents several interesting problems:

1. Existing theory [1]* states that not only is an increasing area required for supersonic flow, but also a diverging physical boundary against which molecular impact can increase downstream motion above maximum molecular motion. Since the area of a parallel-walled, radial passage increases with the radius, can such a passage even though its walls are parallel accelerate air supersonically?

(*Raised arabic numerals refer to bibleography.)

2. If supersonic flow is possible in such a passage, then any induced shock phenomenon would have to manifest itself in a circular pattern. If such discontinuities exist, the problem is to determine the character of the discontinuity and obtain a theoretical explanation of the phenomenon.

3. If it is found that a shock phenomenon does not occur and that no discontinuities exist, then flow in a radial passage would be a method of studying supersonic flow under varying conditions without the complication of shock discontinuities. An example would be the study of friction and boundary layer for supersonic air flow free from the complications of any discontinuities.

This investigation was conducted during the spring term, 1948, with invaluable assistance from and under the guidance of Professor Neil P. Bailey, as a thesis in partial fulfillment of the requirements for the degree of Master of Science at Rensselaer Polytechnic Institute.

EQUIPMENT AND PROCEDURE

The radial flow nozzle (Figure 1) was designed so that the air at its center, the approach to the throat section, was essentially still (less than a Mach Number of 0.20). The physical approach to the throat section was designed on the basis of a conical elliptical approach as per A.S.M.E. standards with a transfer of the ellipse from a conical passage to a radial flow passage. The nozzle was machined of brass and the air passage surface was highly polished.

The radial nozzle and associated equipment were mounted on a lathe bed as shown in the photograph of complete apparatus set-up (Figure 2). The face of the radial nozzle through which the air entered at its center was mounted on a 6" metering compound which contained a standard A.S.M.E. 3/4" metering orifice. The other face was mounted to the lathe carriage which simplified alignment and clearance problems. A close-up of the radial nozzle in operating position is shown in the photograph (Figure 3).

The air which was supplied by a standard 175 CFM, reciprocating, electric-driven, Schramm compressor was water cooled prior to delivery to the metering compound. Air temperature was measured at the metering compound by means of a Weston dial thermometer. A schematic of apparatus is shown in Figure 4.

Static pressure taps consisted of 0.040" holes drilled at the walls and their locations are shown in Figure 1.

Two impact pressures were taken. One consisted of a 0.040" hole drilled at the center of the face attached to the carriage to obtain the total pressure of the air at the center of the nozzle. The other consisted of a 0.035" steel impact tube mounted just at the exit of the radial nozzle (not shown in photographs). All pressure readings were taken with mercury manometers.

The procedure used in aligning the nozzle and obtaining data consisted of the following:

The two faces of the nozzle were carefully aligned for parallelism when separated 0.003" by means of a 0.003" feeler. The operating clearance for the two faces as determined by flow area considerations and as computed in Sample Calculations, Page 22, was measured by using the reverse end of a set of numbered twist drills as "go, no-go" feeler gauges. The clearance was checked in this manner at each operating pressure setting. Runs were made at various overall pressure ratios with the compressor delivering continuously in order to minimize pressure fluctuations. At each setting all nozzle pressure readings were recorded consecutively from one mercury manometer through a manifold. The temperature of the air for each run was recorded after half of all the pressures were read, so that if any fluctuations in temperature occured, the mean temperature would be recorded.

The runs of Set 1 were unknowingly conducted at a different clearance setting for each pressure setting. This clearance change occurred and was resolved as follows:

At the start of Set 1, a clearance of 0.030" was set on the nozzle. The two faces of the nozzle were not physically joined to each other, but one face was secured to the lathe carriage while the other face was fastened to the metering compound which rested on wooden supports secured to the lathe bed. It was felt that the clearance between the two faces would remain constant. However, the resolution of the data of the runs of Set 1 could only be reconciled on the basis of an increasing clearance and flow area. The runs of Set 1 were then duplicated in the laboratory, and the clearance was measured during each run with the "go, no-go" gauges. It was found that the pressure forces on the faces of the nozzle at each run were great enough to cause further clearance separation even though the apparatus was rigidly secured in the lathe bed. The runs of Set 2 were then taken at a constant clearance setting of 0.036". This clearance was kept constant by closing the clearance to 0.036" at each pressure setting and keeping a check on it with the "go, no-go" gauges.

ANALYTICAL DISCUSSION

A complete and concise analytical discussion of the thermodynamics of high velocity air flow is given in Reference 2. That discussion develops theoretical relationships which describe the flow of air in constant area, diverging, and converging passages. It is felt a complete redevelopment of these thermodynamic relationships for a radial passage is unnecessary, except in so far as these relationships deviate from those in conventional passages.

Under the assumptions of reversible flow, i. e., constant total energy, steady flow, and no viscosity or friction effects, the pressure change in a coventional passage is given by $dP = -\rho v dv$. To determine the reversible pressure change in a radial, parallel-walled passage take a pie-shaped element as shown below considering unit depth, and make a summation of pressure forces on an infinitesimal element:

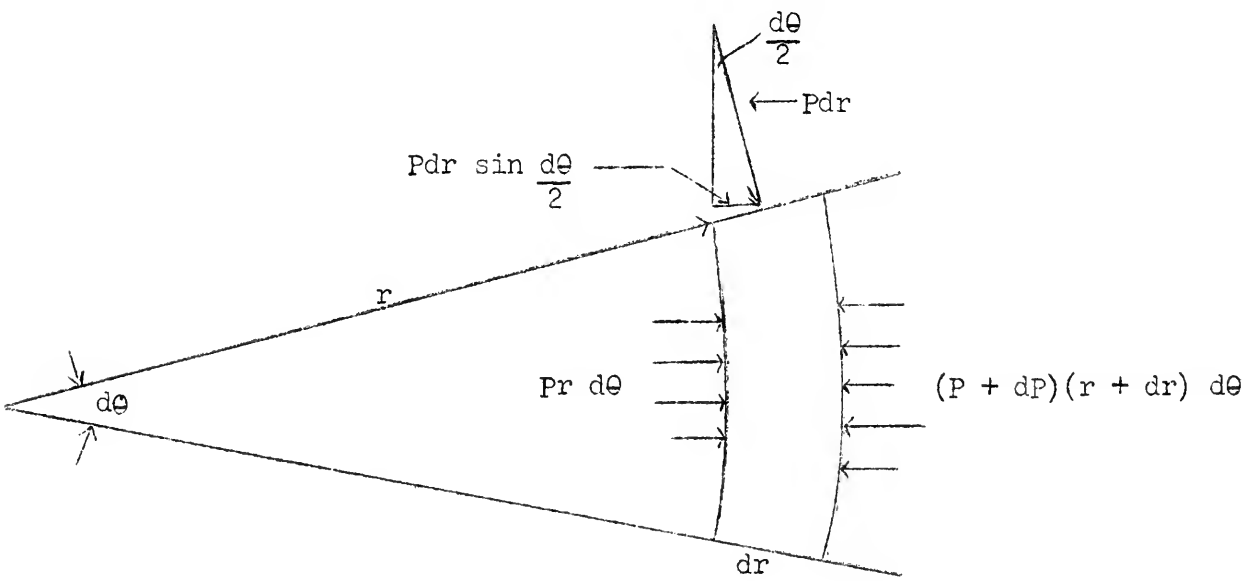

$$\sum \xrightarrow{\qquad} \text{Pressure Forces} - \text{Mass}\left(\frac{dV}{dt}\right) = 0 \quad \ldots\ldots\ldots (1)$$

$$\left[Pr d\theta - (P+dP)(r+dr)\, d\theta + 2\, Pdr \sin\left(\frac{d\theta}{2}\right)\right] - \left[(\rho r d\theta\, dr)\left(\frac{dv}{dt}\right)\right] = 0$$

$$Pr d\theta - (Pr + Pdr + dPr + dPdr)\, d\theta + Pdrd\theta - \rho r d\theta\, vdv = 0$$

$$(-Pdrd\theta - dPrd\theta - dPdrd\theta) + Pdrd\theta - \rho r d\theta\, vdv = 0$$

$$- dPrd\theta - dPdrd\theta - \rho r d\theta\, vdv = 0$$

$$dPr + dPdr + \rho r\, vdv = 0$$

$$dP\,(r + dr) + \rho r\, vdv = 0 \quad \ldots\ldots\ldots\ldots (2)$$

considering second order quantities to be negligible:

$$dPr + \rho r\, vdv = 0$$

$$\therefore dP = -\rho\, vdv \quad \ldots\ldots\ldots\ldots\ldots (3)$$

Equation (3) shows that the reversible pressure change in a radial passage is the same as that for a conventional passage. Therefore, the thermodynamic relationships for reversible flow in a conventional passage applies for reversible flow in a radial passage.

Friction Considerations:

Equation (80) of Reference 2 gives the expression for velocity gradient considering friction and area gradient:

$$\frac{dv}{dx} = v\left[\frac{f\gamma M^2/2m - (1/A)\, dA/dx}{1 - M^2}\right] \quad \ldots\ldots\ldots\ldots (80)$$

The only assumptions in equation (80) are constant total energy and steady flow; therefore, it will apply to a radial passage:

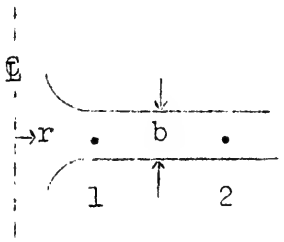

$$\frac{dv}{dr} = v\left[\frac{f\gamma M^2/2m - 1/A \quad dA/dr}{1 - M^2}\right] \quad \ldots\ldots\ldots\ldots\ldots (4)$$

where, $m = \frac{\text{cross section area}}{\text{wetted perimeter}} = \frac{2\pi rb}{4\pi r} = \frac{b}{2}$

$$A = 2\pi rb$$

$$\frac{dA}{dr} = 2\pi b$$

$$\frac{dv}{v} = \frac{f\gamma M^2}{b(1-M^2)}\,dr - \frac{1}{(1-M^2)}\,\frac{dr}{r} \quad \ldots\ldots\ldots\ldots\ldots (5)$$

From the definition of Mach Number and energy equation for no heat transferred or mechanical work done:

$$M^2 = \frac{v^2}{\gamma gRT}$$

differentiating and solving for $\frac{dT}{T}$:

$$\frac{dT}{T} = 2\frac{dv}{v} - 2\frac{dM}{M} \quad \ldots\ldots\ldots\ldots\ldots (6)$$

Energy equation: $\gamma gRdT + (\gamma-1)\,vdv = 0$

$$\frac{dT}{T} = -(\gamma-1)\,M^2\,\frac{dv}{v} \quad \ldots\ldots\ldots (7)$$

solving (6) and (7) for $\frac{dv}{v}$:

$$\frac{dv}{v} = \frac{dM}{M\left[1+\left(\frac{\gamma-1}{2}\right)M^2\right]} \quad \ldots\ldots\ldots\ldots\ldots (8)$$

Equating (5) and (8):

$$\frac{f\gamma}{b}\,dr = \frac{(1-M^2)\,dM}{M^3\left[1+\left(\frac{\gamma-1}{2}\right)M^2\right]} + \frac{dr/r}{M^2} \quad \ldots\ldots\ldots (9)$$

Since M cannot be evaluated in terms of r, equation (6) cannot be integrated to give a direct evaluation of friction factor. However, by rearranging:

$$\frac{f\gamma M^2}{b/r}\,\frac{dr}{r} - \frac{dr}{r} = \frac{(1-M^2)\,dM}{M\left[1+\left(\frac{\gamma-1}{2}\right)M^2\right]}$$

$$\frac{dr}{r} = \frac{dA}{A} = \frac{(1-M^2)\,dM}{M\left[1+\left(\frac{\gamma-1}{2}\right)M^2\right]\left[\frac{f\gamma M^2}{b/r}-1\right]} \quad \ldots\ldots\ldots (10)$$

Equation (10) is in the form in which friction analysis is made for varying area passages of which a full discussion and development is made in Reference 3. Equation (57) of Reference 3 is expressed as follows:

$$\frac{dA}{A} = \frac{(1-M^2)\,dM}{M\left[1+\left(\frac{\gamma-1}{2}\right)M^2\right]\left[\frac{f\gamma M^2}{2c}-1\right]} \quad \ldots\ldots\ldots (57)$$

where $c = \frac{m}{A}\,\frac{dA}{dr}$

for a conical passage c = constant; however, for the radial passage from equation (10), $c = \frac{b}{2r}$, which varies with r.

For a passage where c = constant, equation (57) is integrable but equation (10) is not. However, in Reference 3 curves of equation (57) are plotted with A versus M for various values of f/c. These curves are reproduced in Figure 5. If, for the radial passage, Mach numbers are determined, A and c can be calculated, and from Figure 5 for each A and M, f/c can be obtained. Finally, with the values of f/c, friction factor (f) can be computed.

RESULTS AND DISCUSSION

The first consideration was to determine whether or not the passage produced radial flow. If the flow was radial, then all points of equal radii should have the same pressure. To determine whether this condition existed, three image pressures at the same radii were taken at points 6, 6', and 6" (Figure 1). Many runs in the early stages of the investigation showed very little or no pressure difference between points 6 and 6' indicating good radial flow in the plane of the nozzle. However, a slight pressure gradient was observed between points 6 and 6". It is felt that this gradient was due to the nonsymmetrical entry of air to the nozzle. Table II shows a typical set of these image pressure readings.

During the initial stages of the investigation an external phenomenon occurred which at first was thought to have a bearing on the internal flow. During the initial stages of a run the

air would exit radially, and then for no apparent reason would abruptly fold over the metering compound. When this phenomenon occurred, there was no variation in pressure readings, and any attempt to correlate and control this phenomenon with pressure changes was unsuccessful. Finally, suspecting that the phenomenon was entirely external and was caused by the proximity of the metering compound to the nozzle, an experiment was conducted with a flat plate of the same cross-sectional dimensions as the metering compound, in which this plate was placed so that the nozzle was between the compound and the plate.

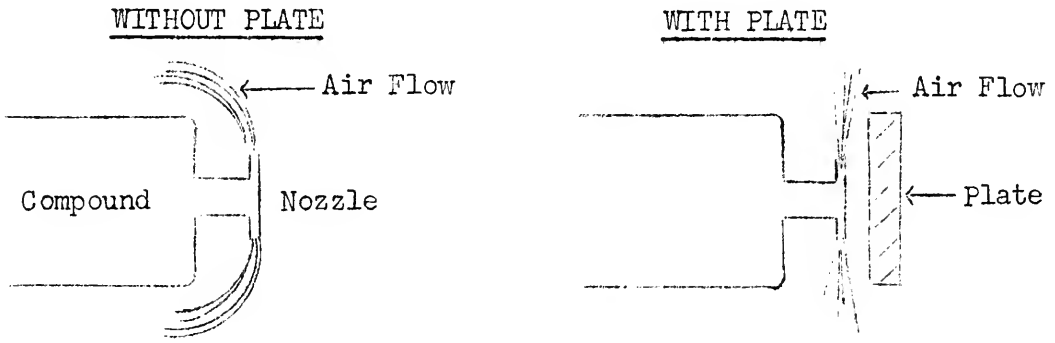

By moving the flat plate closer to the nozzle than the distance from the compound to the nozzle, the air flow was caused to fold abruptly over the flat plate. By moving the plate out so that the distances were equal, the air flow was caused to exit radially. Finally, by moving the plate out so its effect could no longer be felt, the air flow folded back over the compound. These observations showed that the phenomenon was external and was caused by a Magnus or Bernoulli effect.

A total of seven complete sets of runs were made during the investigation of which the data for two are shown in this report. Table I is the data for the runs of Set 1 in which the clearance for each run varied. Table II is the data for runs of Set 2 in which the clearance was held constant, so that the runs indicate different pressure conditions for one radial passage. For runs of Set 1, Table III shows computed results, and Figures 6 through 10 show typical curves of these results. Table IV gives the computed results for the runs of Set 2, and the curves of these results are shown in Figures 11 through 15.

The Mach Number curves (Figures 9 and 14) show that super-acoustic acceleration occurs in all cases when the pressure is sufficient to produce nozzle action. This fact proves that a diverging physical boundary is not required to produce super-acoustic acceleration and that a positive flow area gradient is a necessary and sufficient condition. This observation could be explained on the premise that the gas molecules by impact with themselves can increase downstream motion above maximum molecular motion.

Examination of the curves of Figure 14 shows that the Mach Number curve peaks at the low pressure ratios. This peak increases with overall pressure ratio up to a point where an increase in overall pressure ratio will not change the Mach Number curve as shown by curves 2d and 2e. This observation would indicate that that overall pressure ratio is a critical pressure

ratio for the particular nozzle. The comparison of the pressure ratios for these two runs is as follows:

Run	Overall Pressure Ratio	Throat to Exit
2d	2.93	1.61
2e	2.94	1.61

The curves of Figure 14 look similar to Mach Number curves of any conventional nozzle with the one exception that these curves do not terminate subsonically. In a conventional nozzle when the back pressure is high enough to prevent complete acceleration; a plane shock is produced in which case the flow after the shock is always subsonic, and there is a loss of total pressure. All attempts to analyze the data for plane shock were unsuccessful for two reasons. One was that in only one run did the Mach Number drop to a subsonic value. The other was that any plane shock would require a total pressure loss while as shown in Tables I and II, exit impact readings showed almost complete pressure recovery for all runs. An example is that of Run 2d where a plane shock would require a total pressure of 73.3" Hg. (abs.) at the exit while the impact tube recorded a recovery of 81.7" Hg. (abs.).

One remaining explanation for a diffusion from a supersonic Mach Number is a negative flow area gradient. But physically the area in the radial nozzle increases with radius. However, a boundary layer growth could produce a choking effect and in this particular nozzle cause a change from a positive flow area gradient to a negative gradient. One reason for such an assumption

is that in conventional passages with much larger flow areas, boundary layer thickness is a small first order quantity as compared to the entire flow cross section and can be neglected. However, in this particular passage, due to available air limitations, the cross-sectional flow dimension (clearance) is of the order of 0.036" so that any boundary layer is no longer a negligible small first order quantity.

Since flow areas under investigation were so small, the introduction of any instrumentation into the stream was out of the question. This being the case, the problem of determining the correct stream Mach Numbers became of prime importance. The reasoning and assumptions used in arriving at the best estimate of stream Mach Numbers were as follows:

The total pressure (P_o) was recorded at the center of the face opposite the air entry as shown in Figure 4. This total pressure (P_o) to be used as representing the total pressure of the stream at entry to the nozzle throat was questionable. Since all flow areas up to the throat (point 4) are comparatively large, the weight flow Mach Number at point 4 was considered reliable. From the throat to the exit (4 to 8), the total pressure (P_o) loss was very slight as evidenced by the high recovery of exit impact readings (P_o'). Therefore, a probable Mach Number distribution from throat to exit would correspond to the reversible Mach Number distribution. Weight flow

Mach Numbers based on physical area were proven false by the high exit impact readings. Assuming boundary layer at the throat to be negligible, to have a basis from which to compute boundary layers in the passage, the weight flow Mach Number at the throat (point 4) based on physical area could be considered the reference base for the computation of the Mach Numbers at the remaining points. This assumption of negligible boundary layer at the throat is based on comparatively large flow areas up to the throat, and in addition, a large negative pressure gradient from the center of the passage to the throat. Therefore, the best estimate of stream Mach Numbers would be the weight flow Mach Number at the throat followed by a Mach Number distribution comparable to the reversible Mach Number distribution.

It was on this premise that corrected flow areas were computed which would produce the reversible Mach Numbers attained. The Mach Numbers obtained from weight flow consideration and physical area were then corrected for the new corrected areas which took into account a probable boundary layer.

The validity of this assumption is borne out in the check between the total pressure called for at exit by corrected Mach Number and the actual impact reading at exit.

Run No.	M'_8	P'_{o8} ⟵ As Compared To ⟶	P'_o
1a	.615	37.8	38.1
1b	.954	45.8	45.8
1c	1.060	50.6	51.8
1d	1.130	56.7	57.8
1e	1.195	63.3	64.1
1f	1.220	68.0	69.8

Typical Mach Number curves showing the comparisons between reversible Mach Number, weight flow Mach Number, and corrected weight flow Mach Number, are shown in Figures 7 and 12.

The probable boundary layer picture under this assumption is shown in Figures 10 and 15. Examination of these boundary layers in Figure 15 shows that the boundary layer is stabilized for a greater distance and its growth is delayed in progressing from Run 2a to Run 2e. The strengthening conviction in this boundary layer picture is that it conforms well with boundary layer theory. Theory states that a negative pressure gradient stabilizes boundary layer growth, whereas, a positive pressure gradient de-stabilizes boundary layer and causes its growth. Comparison of Figure 15 with the pressure curves of Figure 11 shows that while the pressure gradient is negative the boundary layer is thin and stable, but as soon as the pressure gradient changes from negative to positive boundary layer growth begins.

A recent study[4] of friction factors for supersonic flows in passage showed how difficult it is to isolate the pure friction

problem from both shock phenomenon and boundary layer. In that study much effort was expended in designing a passage with minimum shocks, and even so, the results for friction coefficients were inconsistent and not conclusive. In the radial passage, the friction factor results, when taking into account the probable boundary layer, are shown in Figures 8 and 13. These friction factors can be considered constant in comparison to the variation obtained when net area due to boundary layer is not taken into account. These results would indicate that friction factors, when divorced from shock losses and boundary layer, are probably constant and a function of the boundary surface.

It is concluded then, that flow in a radial, parallel-walled passage, with flow clearance the same order of magnitude as boundary layer thickness, is continuous under all pressure conditions. The first impression is that all previous knowledge shows that in any air flow at supersonic velocities, shock discontinuities occur when certain flow conditions are not met. However, it is conceivable that in a passage where a flow dimension is not large enough to permit the build up of a finite shock discontinuity, a boundary layer alone could satisfy all flow conditions. One of the most interesting problems in this investigation could not be studied because of air limitations in the laboratory. That problem is, "How would air flow adjust itself to different pressure conditions in a radial, parallel-walled passage with flow clearance of such magnitude that boundary layer thickness may be neglected in flow area computations?"

It is felt that the data obtained in this investigation was insufficient to make the results and conclusions obtained conclusive. However, it would appear that fundamental supersonic air flow studies in which discontinuities are undesirable could be advantageously carried out in a radial, parallel-walled passage with small flow clearance. Especially of interest is the study of boundary layers under supersonic conditions without the complication of shock discontinuities.

CONCLUSIONS

A positive area gradient without a diverging boundary will produce super-acoustic acceleration.

Air flow in a radial, parallel-walled passage, with flow clearance the same order of magnitude as boundary layer thickness, is continuous under all pressure conditions.

Friction factor for the particular passage in this investigation can be considered constant regardless of whether air flow in the passage is accelerating or diffusing.

Since the study of friction factors and boundary layer in diffusing passages at high flow velocities has been a problem of great interest, it is felt that a radial, parallel-walled passage with small flow clearance can be used to advantage in such studies and in other fundamental flow studies where discontinuities are undesirable.

RECOMMENDATIONS

Sufficient data should be taken to make the results conclusive. One method of obtaining more data would be to instrument the face of the nozzle with static pressure taps separated 0.01" in radius. This instrumentation could be accomplished by drilling smaller pressure holes and spacing them in a spiral pattern about 15° apart, each one increasing in radius 0.01". This pattern would give a total of twenty-four static pressure taps from throat to exit. Such instrumentation would not only be desirable but necessary in conducting a boundary layer study.

To divorce flow phenomenon from boundary layer effects, this investigation should be conducted under conditions where available air is sufficient to permit flow areas such that boundary layer variations can be considered to have negligible affect on flow areas used in computations.

NOMENCLATURE

$M_{(rev)}$ = reversible Mach Number based on total pressure (P_o) constant.

M = Mach Number computed by weight flow on basis of physical area.

M' = Mach Number computed by weight flow on basis of corrected flow area due to probable boundary layer.

A = flow area, sq. in.

A' = net flow area, sq. in., corrected for probable boundary layer.

b = geometric clearance between the two walls of the passage, inches.

b' = net flow clearance corrected for boundary layer thickness, inches.

r = radius, inches.

γ = adiabatic gas constant, 1.395 for dry air at 80° F.

g = acceleration of gravity = 32.2 ft./sec.^{2}

R = gas constant for air = 53.3 ft. lbs./lb., ° Rankine.

P = absolute static pressure, lbs./sq. ft. or inches Hg.

P_o = total pressure, lbs./sq. ft. or inches Hg.

T = static temperature, ° Rankine.

T_o = total temperature, ° Rankine.

ρ = mass density, slugs/cu. ft.

W = air flow, lbs./sec.

Q = air flow, cu. ft./min. at standard conditions.

v = velocity, ft./sec.

m = hydraulic radius, ft.

f = flow friction factor.

SAMPLE CALCULATIONS

I. Design of flow dimensions for radial, parallel-walled passage:

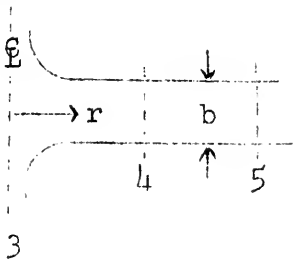

Assumptions: $Q = 175$ CFM.
$w = 0.20$ lb./sec.
$T_o = 550°$Rankine.
$P_o = 80"$ Hg. Abs. $= 39.2$ psia.
$M_4 = 1.0$
$r_4 = 1.0"$
Steady flow.
Constant total energy.

1. Determination of wall clearance (b):

For air flow in any passage, equation $(47)^2$ states:

$$\frac{w\sqrt{T_o}}{PA} = M\sqrt{\frac{\gamma g}{R}\left(1 + \frac{\gamma-1}{2} M^2\right)}$$

$$\frac{w\sqrt{T_o}}{P_4 A_4} = 1.004$$

$$A_4 = \frac{w\sqrt{T_o}}{1.004\ P_4}$$

Assuming reversible flow from (3) to (4), equation $(24)^2$ states:

$$\frac{P_o}{P} = \left[1 + \left(\frac{\gamma-1}{2}\right) M^2\right]^{\frac{\gamma}{\gamma-1}}$$

$$\frac{P_o}{P_4} = 1.890$$

$$P_4 = \frac{39.2}{1.89} = 20.7$$

$$A_4 = \frac{.20\sqrt{550}}{1.004 \times 20.7} = .225$$

$$A_4 = 2\pi r_4 b$$

$$b = .036"$$

2. Determination of maximum radius (r_8) to produce $M_8 = 1.6$, under the assumption of ideal flow from (4) to (8):

From equation (36)[2] and Figure 3[2]:

$$\frac{A_4}{A_{M=1}} = 1.0$$

$$\frac{A_8}{A_{M=1}} = 1.25$$

$$\therefore \frac{A_8}{A_4} = \frac{r_8}{r_4} = 1.25$$

$$\therefore r_8 = 1.25"$$

II. Resolution of data from Tables I and II:

Taking point 6 of Run 2c to illustrate method used in arriving at results shown in Tables III and IV.

Sample Data:

$P_2 = 67"$ Hg. Abs. $\qquad \frac{P_1}{P_2} = 1.052$

$P_6 = 24.2$ Hg. Abs.

$P_o = 67.5$ Hg. Abs. $\qquad A_2 = .4418$ in.^{2}

$P_o' = 66.7$ Hg. Abs. $\qquad A_6 = .250$ in.^{2}

$T_o = 561$ °Rankine.

1. To determine M_2 assume reversible flow through metering orifice, and assume $M_1 = 0$:

$$\frac{P_1}{P_2} = \frac{P_o / P_2}{P_o / P_1} = \frac{P_o / P_2}{1} = 1.052$$

From Figure $(2)^2$ – $M_2 = .270$:

2. To determine W:

From Figure $(4)^4$ – $\dfrac{w\sqrt{T_o}}{P_2 \; A_2} = .250$:

$$\therefore W = .153 \text{ lbs./sec.}$$

3. To determine M_6:

$$\frac{w\sqrt{T_o}}{P_6 \; A_6} = \frac{w\sqrt{T_o}}{P_2 \; A_2} \times \frac{P_2}{P_6} \times \frac{A_2}{A_6} = 1.222$$

From Figure $(4)^2$ – $M_6 = 1.180$:

4. To determine M_6 (reversible):

$$\frac{P_o}{P_6} = 2.790$$

From Figure $(2)^2$ – M_6 (rev)= 1.305

5. To determine net flow area and resultant probable boundary layer required to produce reversible Mach Number:

From Figure $(3)^2$ – $A_6'/A_M = 1 = 1.069$

$A_4/A_M = 1 = 1.002$

$$\frac{A_4}{A_6'} = .938$$

$$A_6' = .240$$

$$b_6' = .0346"$$

probable boundary layer thickness = $\frac{.036 - .0346}{2} = .0007"$

6. To determine Mach Number (M_6') corrected for boundary layer:

$$\frac{w\sqrt{T_o}}{P_6 A_6'} = \frac{w\sqrt{T_o}}{P_6 A_6} \times \frac{A_6}{A_6'} = 1.273$$

From Figure (4)^2 - $M_6' = 1.22$

7. To determine friction factor (f):

From Figure 14 of this report, M = 1 at r = 1.0225,

$$\therefore A'_{M=1} = .227$$

and $\frac{A_6'}{A_{M=1}'} = 1.057$

From Figure 5 of this report for $M_6' = 1.22$ and $\frac{A_6'}{A_{M=1}} = 1.057$,

f/c = 37

$$c = \frac{b'}{2r} = .01565$$

$$\therefore f = .0058$$

BIBLEOGRAPHY

1. Bailey, N. P. — Principles of Heat Engineering, John Wiley and Sons, 1942, Pages 151-152, Chapter 12.

2. Bailey, N. P. — The Thermodynamics of Air at High Velocities (In Journal of Aeronautical Sciences, Volume II, No. 3, July 1944)

3. Bailey, N. P. — The Effects of Friction on High Velocity Flow of Air in Constant Area Channels, in Diffusers, and in Nozzles (General Electric data Folder No. 45259, October 13, 1942)

4. Keenan, J. H. and Neumann, E. P. — Measurement of Friction in a Pipe for Subsonic and Supersonic Flow of Air (In Journal of Applied Mechanics, A.S.M.E. Transactions, Volume 68, Page A-91, 1946)

TABLE I

Laboratory Data - Set 1

Barometer: 29.80" Hg.

All pressure readings in inches Hg. guage.

Run No.	P_2	(P_1-P_2)	P_3	P_4	P_5	T_2 (° F.)
1a	8.2	1.6	7.6	-2.3	-2.6	80
1b	16.2	2.6	15.2	-3.7	-8.4	93
1c	22.2	3.3	20.9	-0.8	-5.9	99
1d	28.2	4.2	26.3	+2.1	-3.4	100
1e	34.2	5.4	31.8	4.8	-1.0	98
1f	40.2	6.8	37.1	7.6	+0.5	99

Run No.	P_6	P_8	P_o	P'_o	b
1a	-2.2	-0.5	8.5	8.3	0.033"
1b	-9.2	-4.1	16.4	16.0	0.035
1c	-9.4	-4.9	22.5	22.0	0.038
1d	-8.9	-4.3	28.5	28.0	0.040
1e	-7.2	-3.6	34.8	34.3	0.043
1f	-5.4	-2.6	40.6	40.0	0.0465

TABLE II

Laboratory Data - Set 2

Barometer: 30.40" Hg.

b = 0.036" (constant)

All pressure readings in inches Hg. guage.

Run No.	P_2	(P_1-P_2)	P_3	P_4	P_5	P_6
2a	9.6	2.1	8.6	-5.0	-6.2	-5.3
2b	21.6	2.7	20.5	-0.3	-7.0	-8.5
2c	36.6	3.5	35.2	+7.7	-0.2	-6.2
2d	52.6	4.1	50.9	15.4	+7.3	-0.8
2e	59.6	4.3	57.5	18.9	10.5	+1.9

Run No.	T_2(°F.)	P_6'	P_6''	P_7	P_8	P_o	P_o'
2a	92	-5.1	-5.2		-1.7	9.8	9.7
2b	100	-8.7	-8.3		-4.4	21.8	21.3
2c	101	-6.4	-6.2		-1.7	37.1	36.3
2d	103	-0.4	+0.8	-1.5	-1.9	53.0	51.3
2e	103	+2.4	+3.4	+1.2	+0.3	60.0	58.0

TABLE III

Computation Results - Set 1

$M_{(rev)}$ - Reversible Mach Numbers based on total pressure (P_o) constant.

M - Mach Number computed by weight flow on basis of physical area.

M' - Mach Number computed by weight flow on basis of corrected flow area due to probable boundary layer. Flow area corrected by area requirements called for by reversible Mach Numbers.

Run No.	P_4(abs.)	M_4(rev)	M_4	M'_4	b'_4	f_4
1a	27.5"	.707	.688	.688	.033"	--
1b	26.1	.945	.940	.940	.035	--
1c	29.0	.955	.930	.930	.038	--
1d	31.9	.970	.957	.957	.040	--
1e	34.6	.985	.971	.971	.043	--
1f	37.4	.995	.966	.966	.0465	--

TABLE III (continued)

Run No.	P_5(abs.)	M_5(rev)	M_5	M'_5	b'_5	f_5
1a	27.2"	.718	.670	.700	.0314"	—
1b	21.4	1.11	1.08	1.105	.034	—
1c	23.9	1.12	1.065	1.092	.0370	.00445
1d	26.4	1.13	1.09	1.100	.0391	.00472
1e	28.8	1.14	1.10	1.120	.042	.00100
1f	30.3	1.165	1.12	1.135	.0459	.0056

Run No.	P_6(abs.)	M_6(rev)	M_6	M'_6	b'_6	f_6
1a	27.6"	.700	.617	.680	.0298"	—
1b	20.6	1.14	1.05	1.130	.032	—
1c	20.4	1.24	1.15	1.210	.0357	.00405
1d	20.9	1.305	1.25	1.290	.0385	—
1e	22.6	1.325	1.27	1.300	.0417	.00472
1f	24.4	1.330	1.265	1.290	.0452	.0051

TABLE III (continued)

Run No.	P_8(abs.)	M_8(rev)	M_8	M'_8	b'_8	f_8
1a	29.3"	.630	.535	.615	.0286"	—
1b	25.7	.958	.802	.954	.02865	—
1c	24.9	1.087	.895	1.060	.0313	.0052
1d	25.5	1.155	.980	1.130	.0338	.0077
1e	26.2	1.210	1.045	1.195	.0365	.0075
1f	27.2	1.250	1.075	1.220	.0399	.0041

Run No.	M_2(rev)	M_3	W	P'_{08}/P_8	P'_{08}	P'_0
1a	.240	.132	.079	1.290	37.8	38.1
1b	.285	.165	.112	1.785	45.8	45.8
1c	.300	.175	.1325	2.03	50.6	51.8
1d	.320	.190	.1585	2.22	56.7	57.8
1e	.345	.202	.1885	2.42	63.3	64.1
1f	.365	.220	.219	2.50	68.0	69.8

TABLE IV

Computation Results - Set 2

Run No.	P_4 (abs.)	M_4 (rev)	M_4	M'_4	b'_4	f_4
2a	25.4"	.836	.792	.792	.036"	—
2b	30.1	.925	.860	.860	.036	—
2c	38.1	.945	.875	.875	.036	—
2d	45.8	.965	.895	.895	.036	—
2e	49.3	.970	.900	.900	.036	—

Run No.	P_5 (abs.)	M_5 (rev)	M_5	M'_5	b'_5	f_5
2a	24.2"	.883	.797	.833	.0342"	—
2b	23.4	1.135	1.035	1.058	.0351	.0085
2c	30.2	1.136	1.035	1.055	.0351	.0085
2d	37.7	1.130	1.025	1.047	.0351	.0085
2e	40.9	1.130	1.020	1.040	.0352	.0085

TABLE IV (continued)

Run No.	P_6(abs.)	M_6(rev)	M_6	M'_6	b'_6	f_6
2a	25.1"	.848	.728	.802	.0322"	--
2b	21.9	1.185	1.037	1.110	.0332	.0060
2c	24.2	1.305	1.180	1.220	.0346	.0058
2d	29.6	1.310	1.188	1.225	.0346	.0058
2e	32.3	1.306	1.178	1.217	.0346	.0063

Run No.	P_7(abs.)	M_7(rev)	M_7	M'_7	b'_7	f_7
2d	28.9"	1.328	1.15	1.240	.0328"	.0055
2e	31.6	1.323	1.14	1.235	.0328	.0055

TABLE IV (continued)

Run No.	P_8(abs.)	M_8(rev)	M_8	M'_8	b'_8	f_8
2a	28.7"	.710	.585	.670	.0313"	--
2b	26.0	1.075	.820	.975	.0296	--
2c	28.7	1.175	.940	1.095	.0302	.0075
2d	28.5	1.337	1.132	1.247	.0319	.0053
2e	30.7	1.340	1.135	1.248	.0320	.0055

Run No.	M_2(rev)	M_3	W	P'_{o8}/P_8	P'_{o8}	P'_o
2a	.268	.155	.092	1.350	38.8	40.1
2b	.269	.155	.119	1.845	48.0	51.7
2c	.270	.155	.153	2.120	61.0	66.7
2d	.268	.155	.189	2.580	73.5	81.7
2e	.267	.155	.204	2.590	79.6	88.4

FIGURE 1

RADIAL FLOW NOZZLE

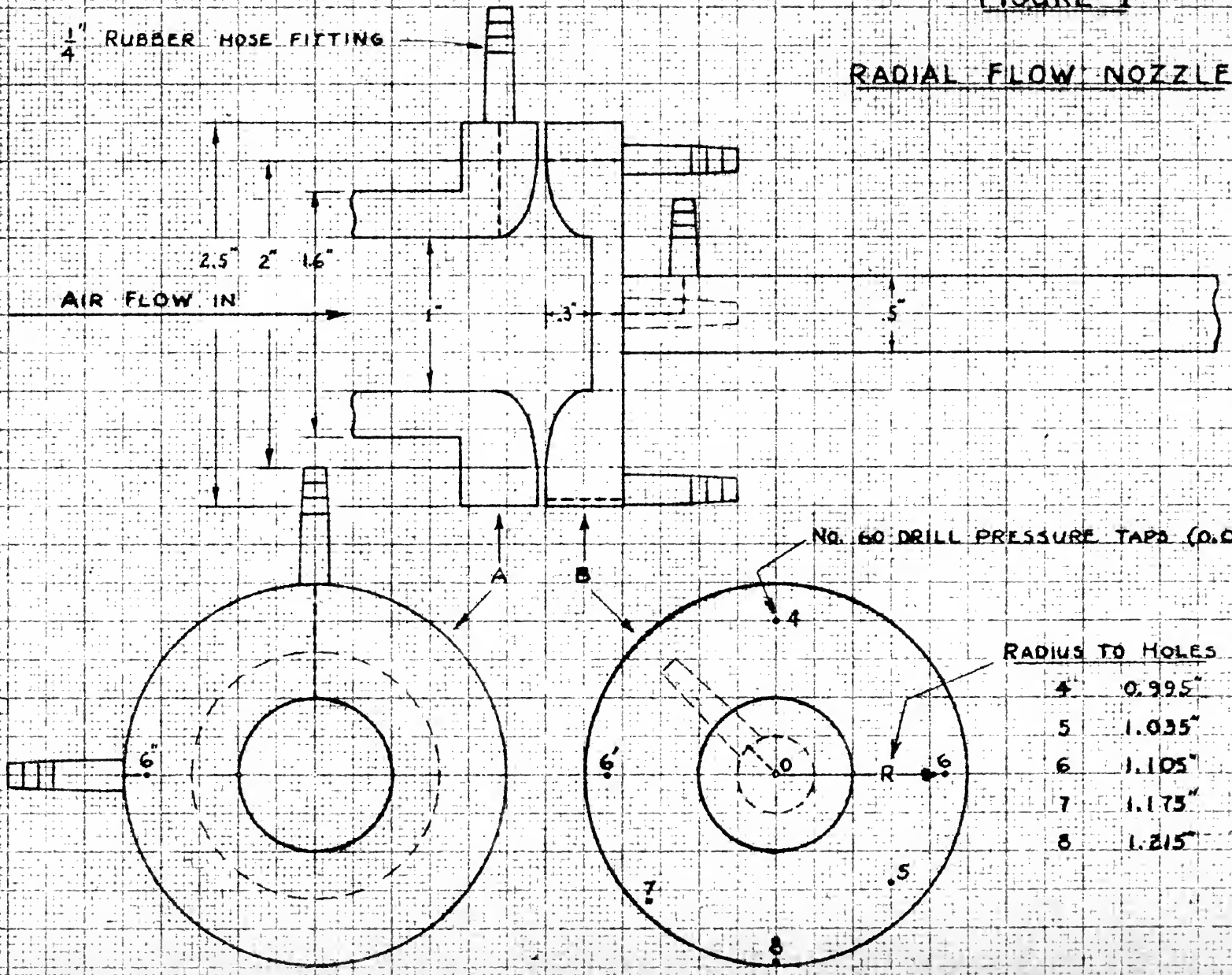

RADIUS TO HOLES	
4	0.995"
5	1.035"
6	1.105"
7	1.175"
8	1.215"

FULL SCALE

FIGURE 2

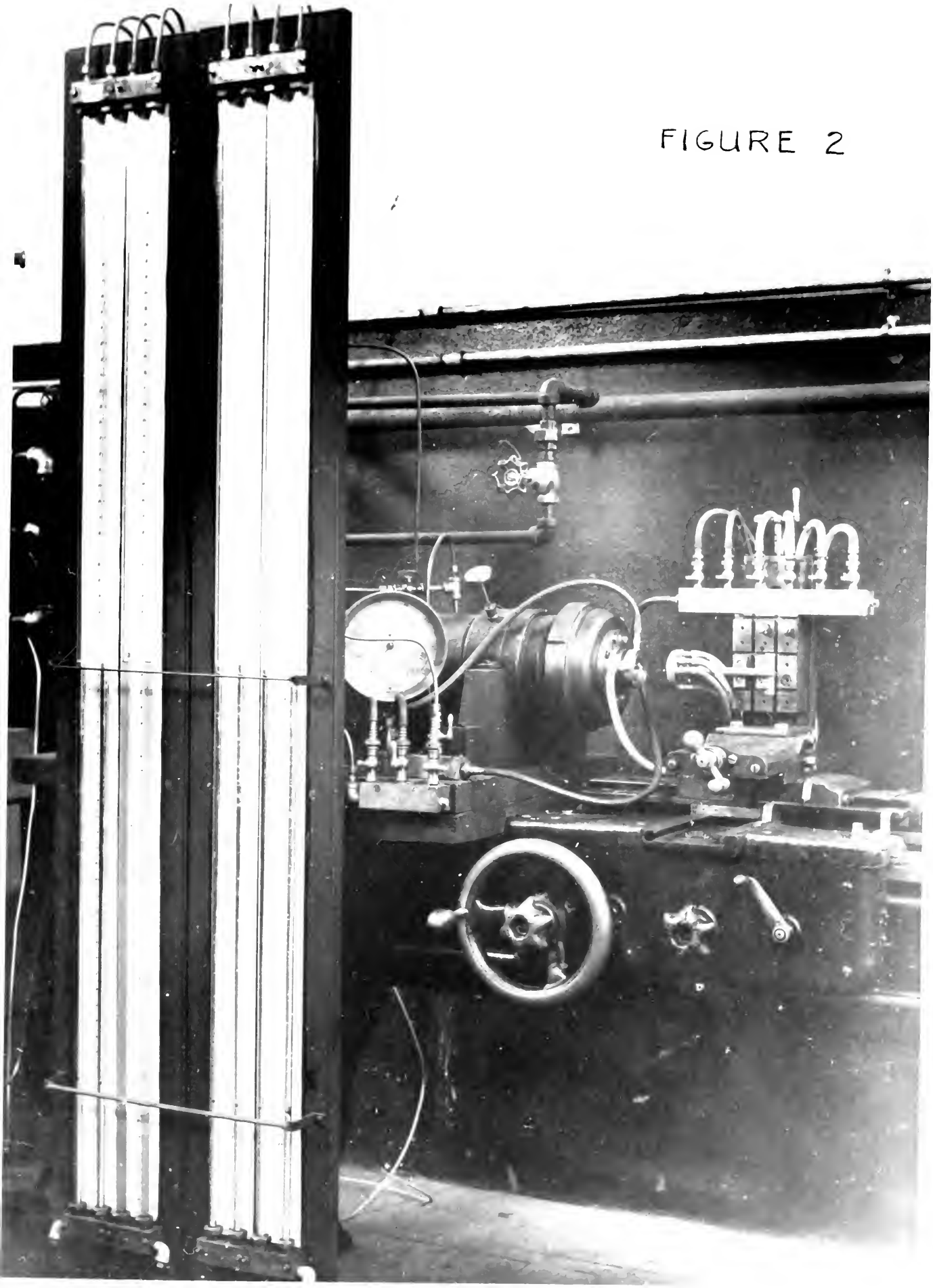

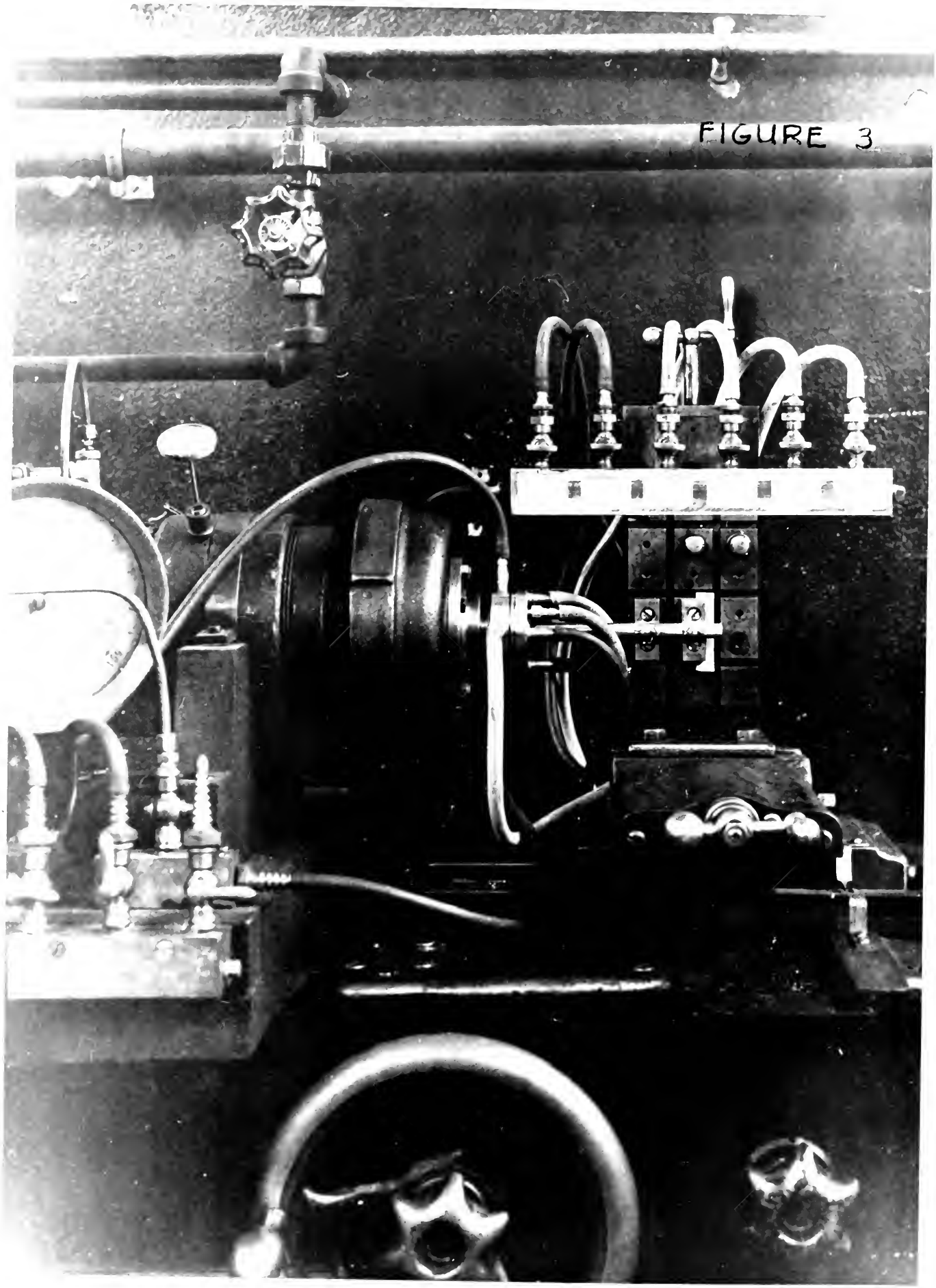

FIGURE 3

FIGURE 4

SCHEMATIC OF APPARATUS

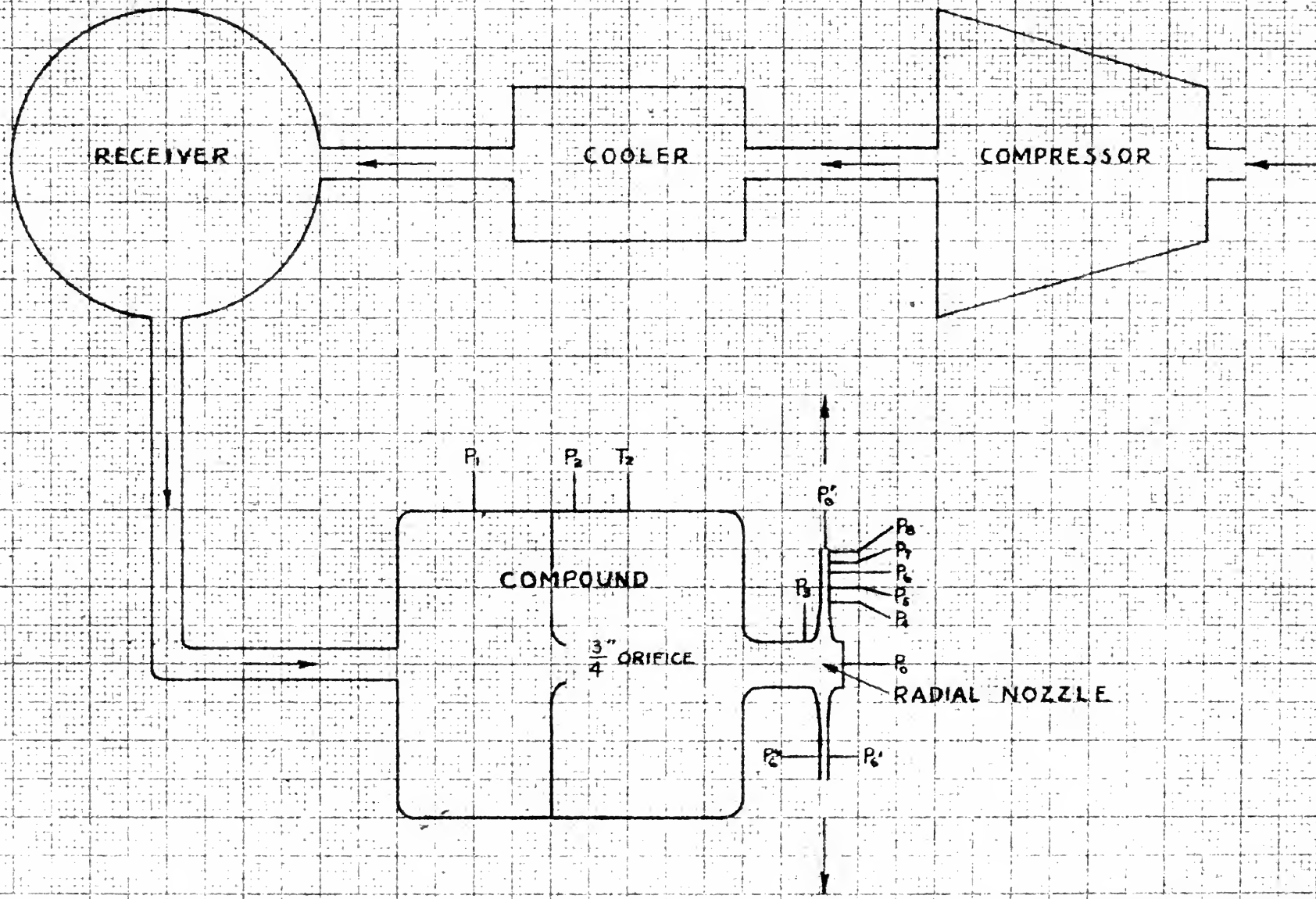

FIGURE 5

EFFECT OF FRICTION ON THE CHANGE IN MACH NO. OCURRING IN SUPER ACOUSTIC NOZZLES

$$\int \frac{dA}{A} = \int \frac{(1+M^2)\,dM}{M\left[1+\left(\frac{\gamma-1}{2}\right)M^2\right]\left[\frac{f\gamma M^2}{2c}-1\right]}$$

$$c = \frac{m}{A}\frac{dA}{dR} = \frac{b}{2R}$$

m = HYDRAULIC RADIUS

f = FRICTION COEFF. BASED ON m

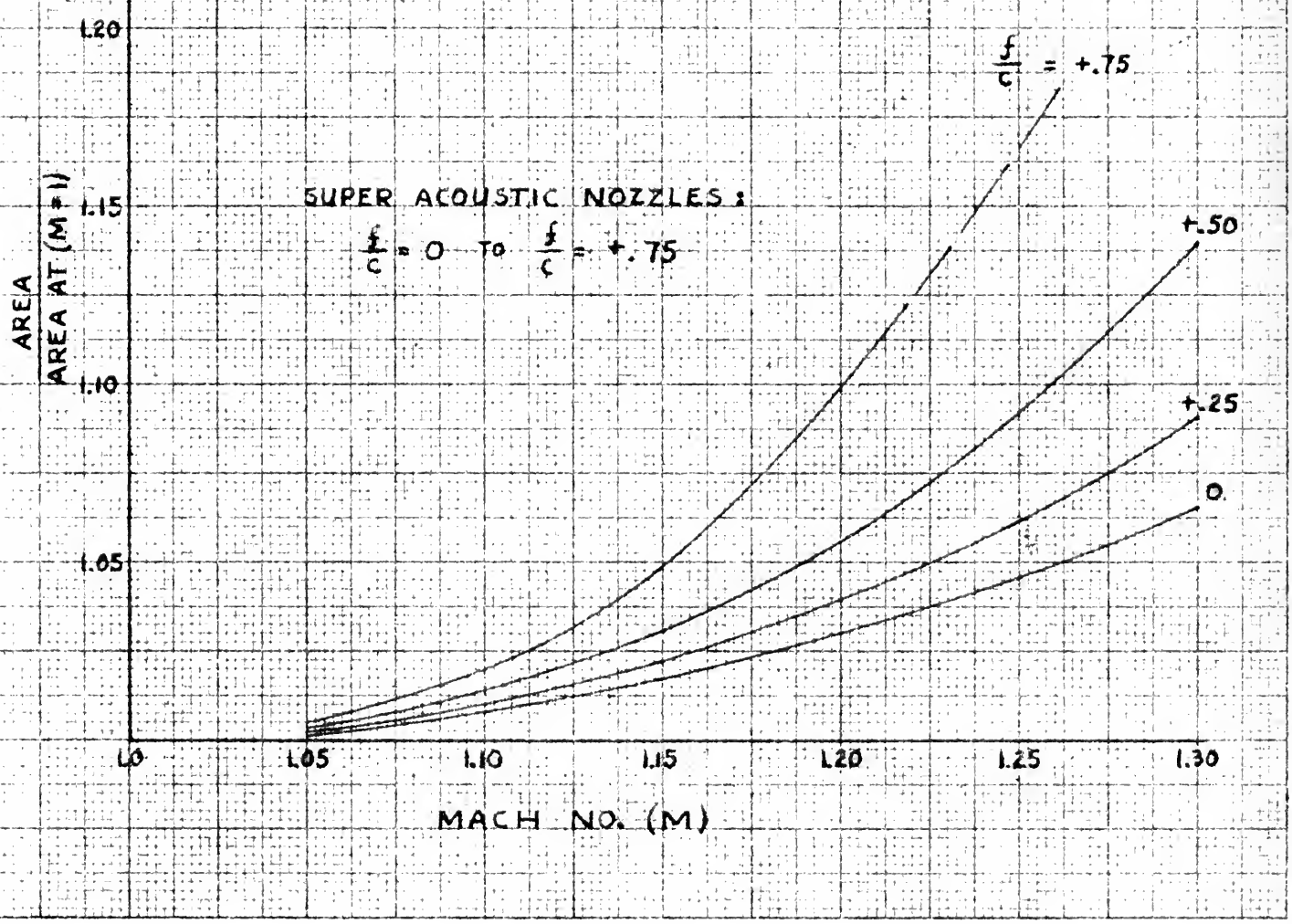

FIGURE 6

STATIC PRESSURE CURVES FOR RUNS OF SET 1

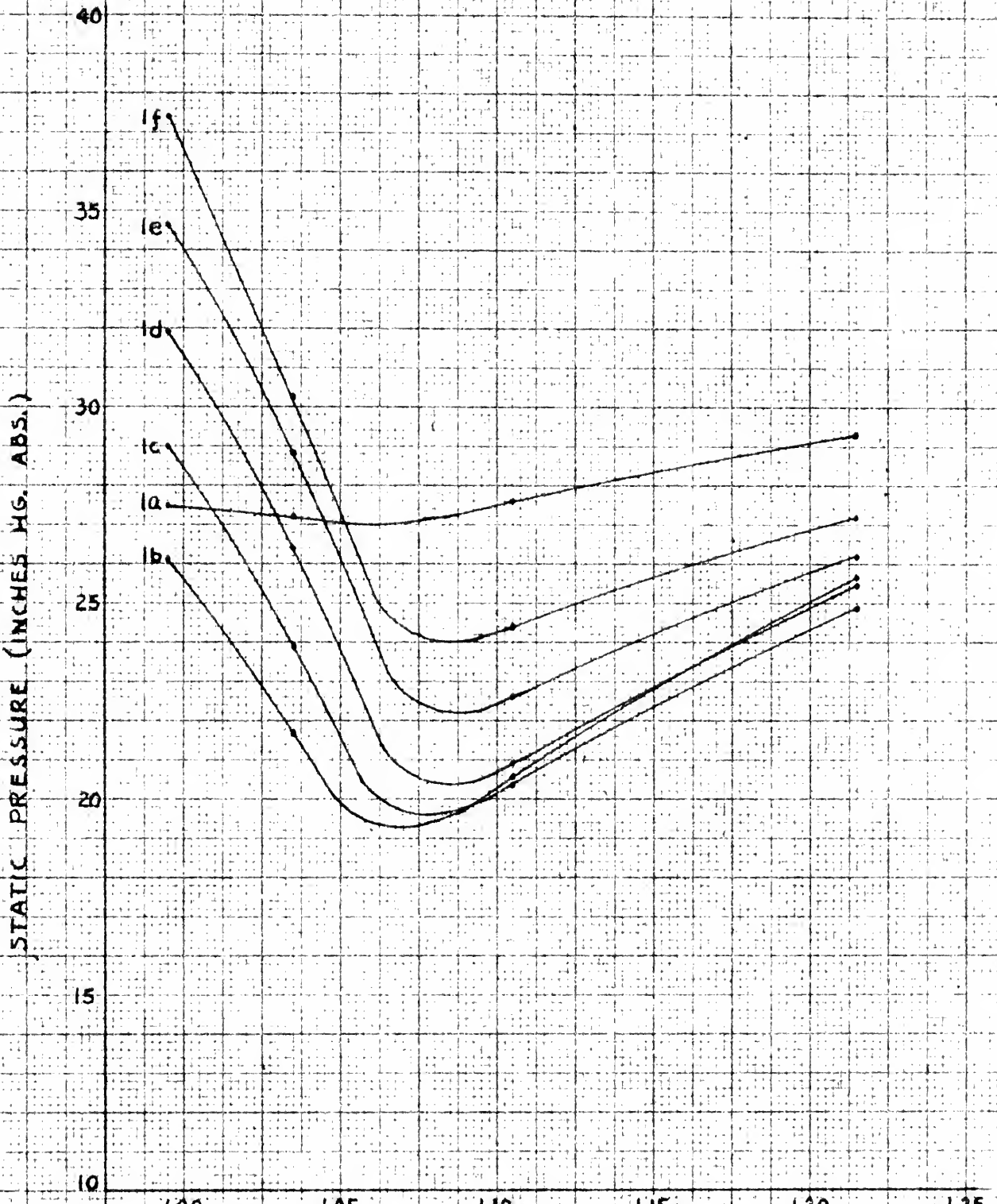

FIGURE 7

TYPICAL MACH NUMBER CURVES
RUN 1f OF SET 1 (P_o = 70" Hg ABS.)

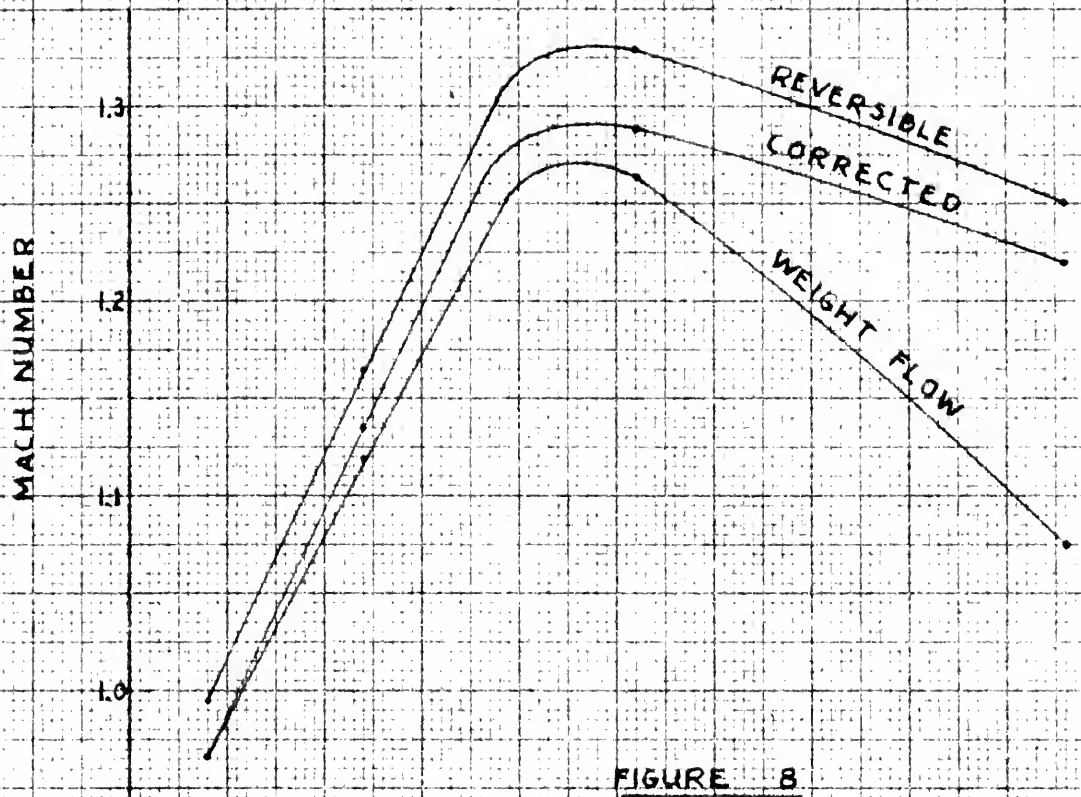

FIGURE 8

FRICTION FACTORS FOR RUNS OF SET 1

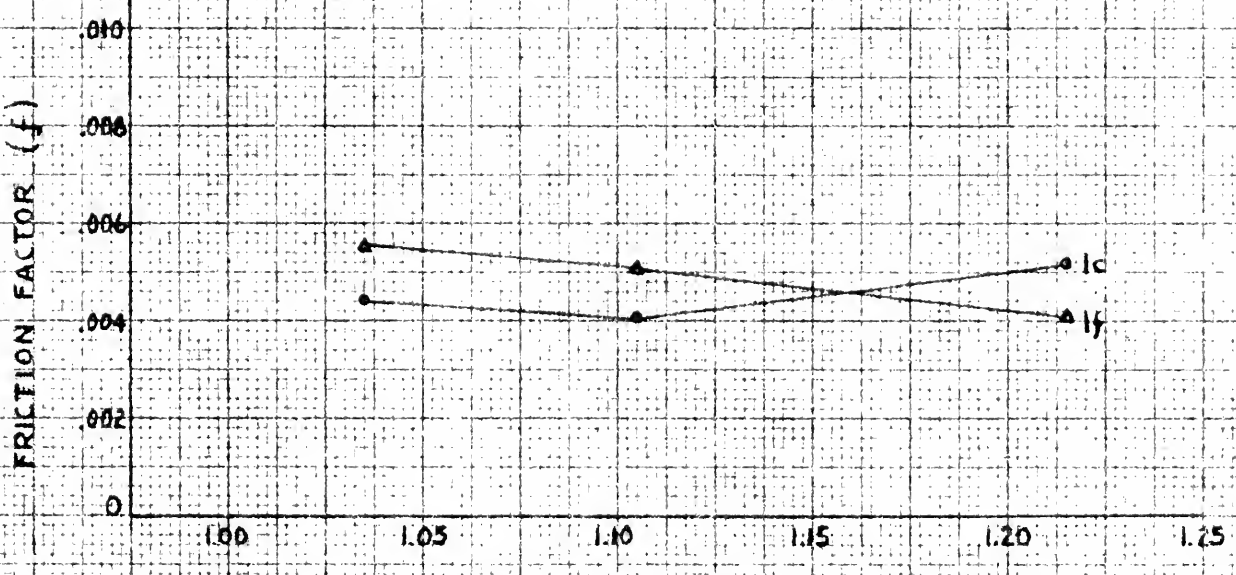

FIGURE 9

CURVES OF CORRECTED MACH NO. (M') VERSUS RADIAL DISTANCE FOR RUNS OF SET 1 WITH VARYING CLEARANCE (b)

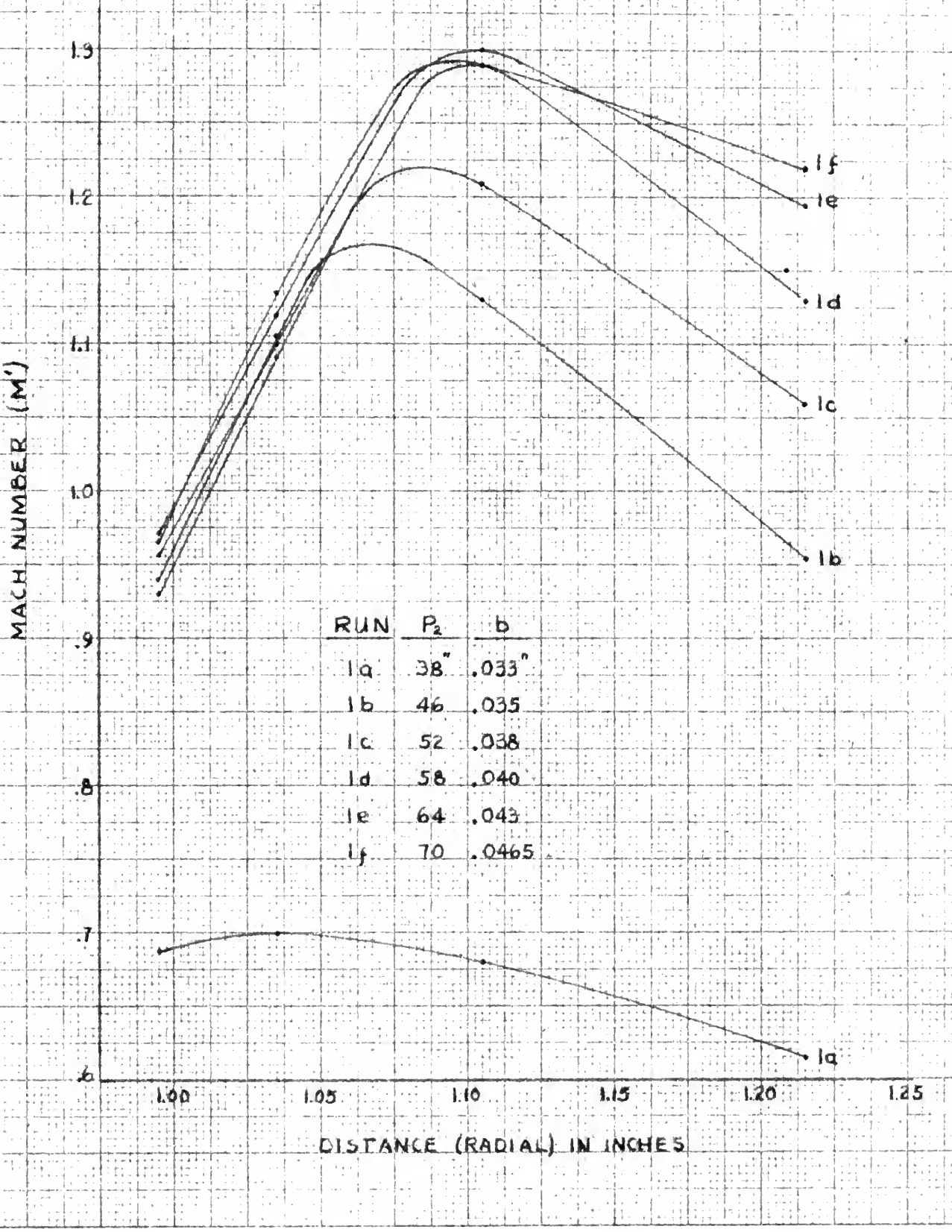

RUN	P_2	b
1a	38"	.033"
1b	46	.035
1c	52	.038
1d	58	.040
1e	64	.043
1f	70	.0465

FIGURE 10

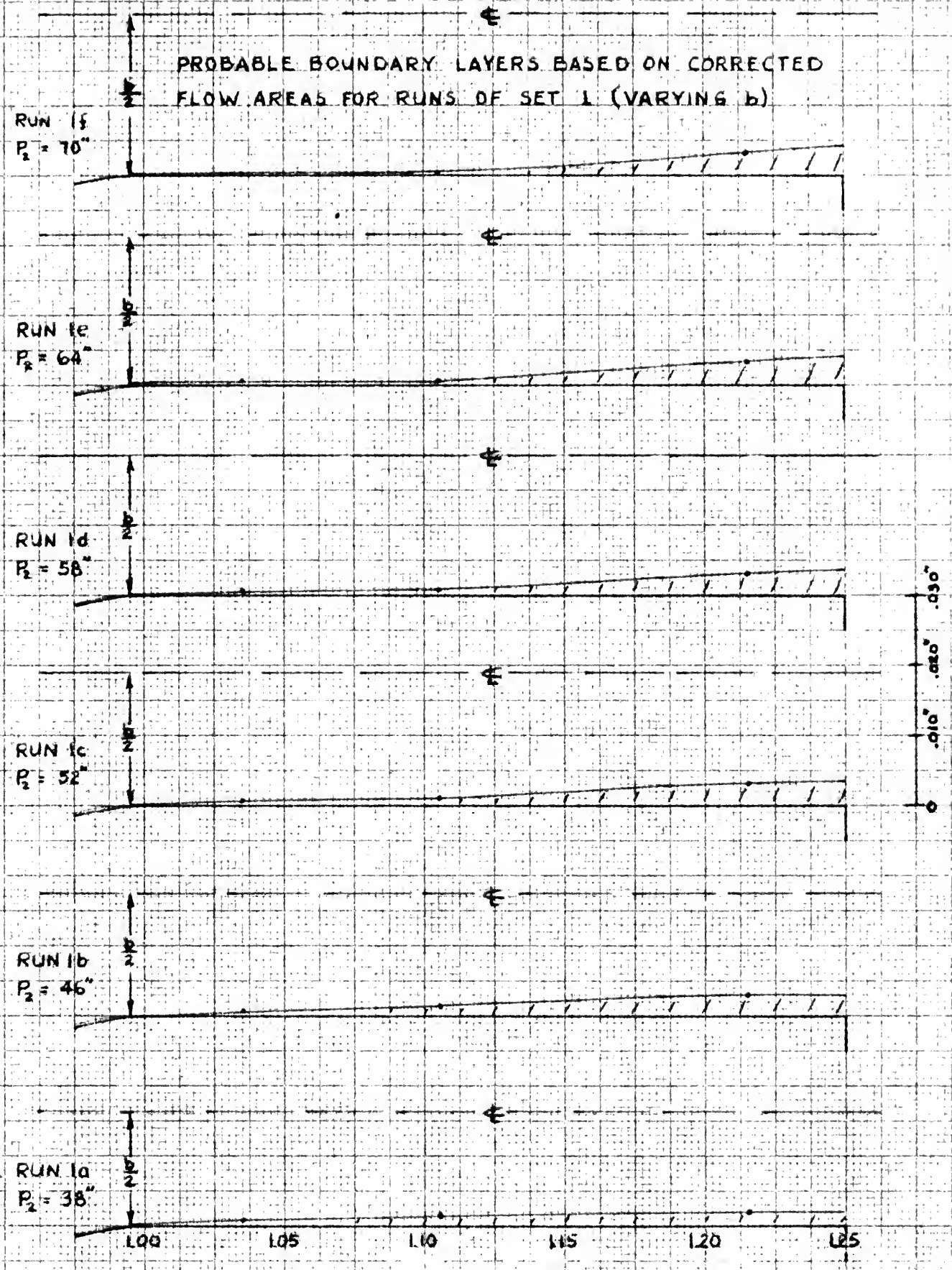
PROBABLE BOUNDARY LAYERS BASED ON CORRECTED FLOW AREAS FOR RUNS OF SET 1 (VARYING b)
RUN 1f
P₂ = 70"
RUN 1e
P₂ = 64"
RUN 1d
P₂ = 58"
RUN 1c
P₂ = 52"
RUN 1b
P₂ = 46"
RUN 1a
P₂ = 38"
b/2
.030"
.020"
.010"
0
1.00
1.05
1.10
1.15
1.20
1.25
DISTANCE (RADIAL) IN INCHES

FIGURE 11

STATIC PRESSURE CURVES FOR RUNS OF SET 2

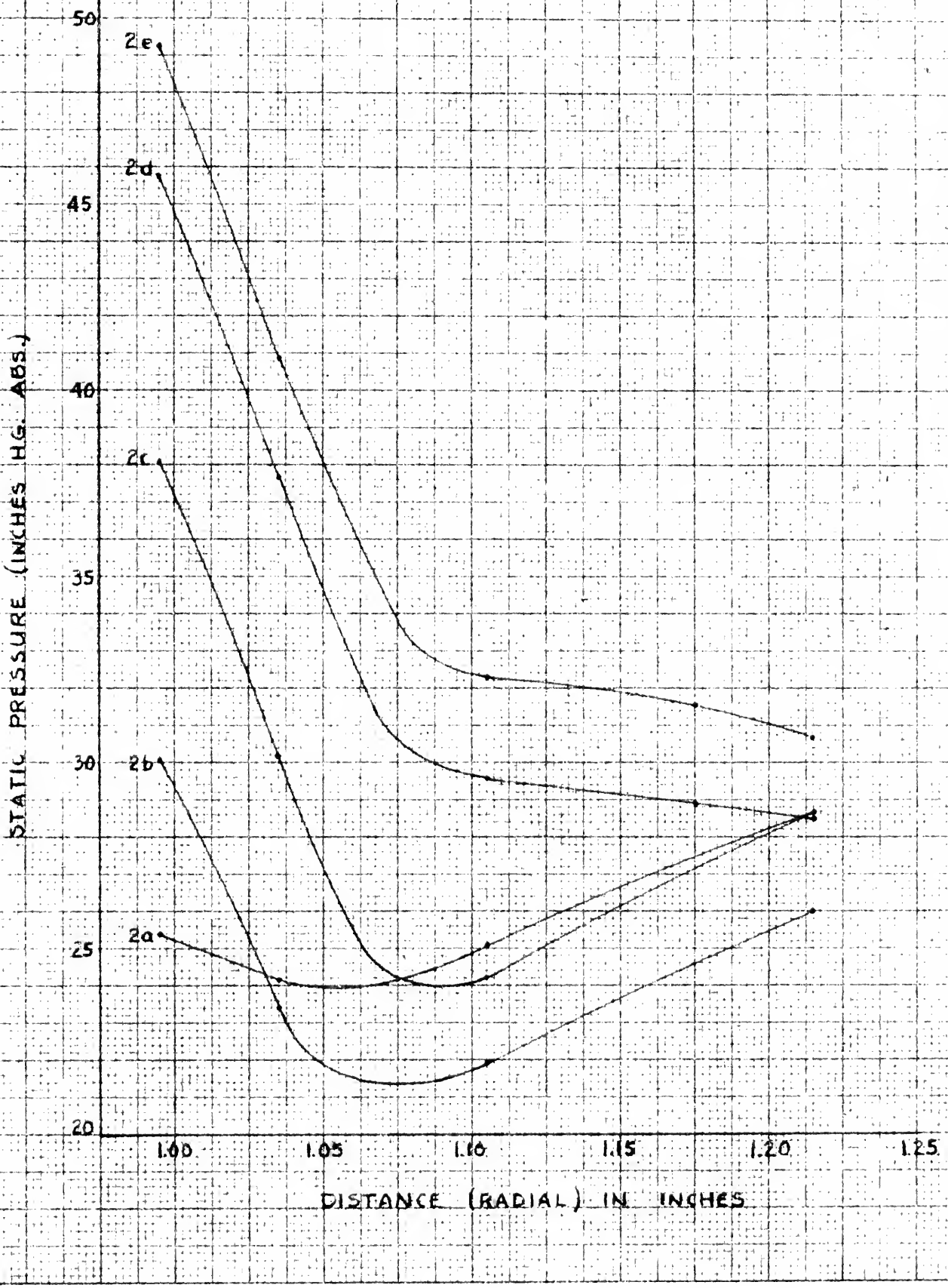

FIGURE 12

TYPICAL MACH NUMBER CURVES
RUN 2d OF SET 2 (P_4 = 83" HG. ABS.)

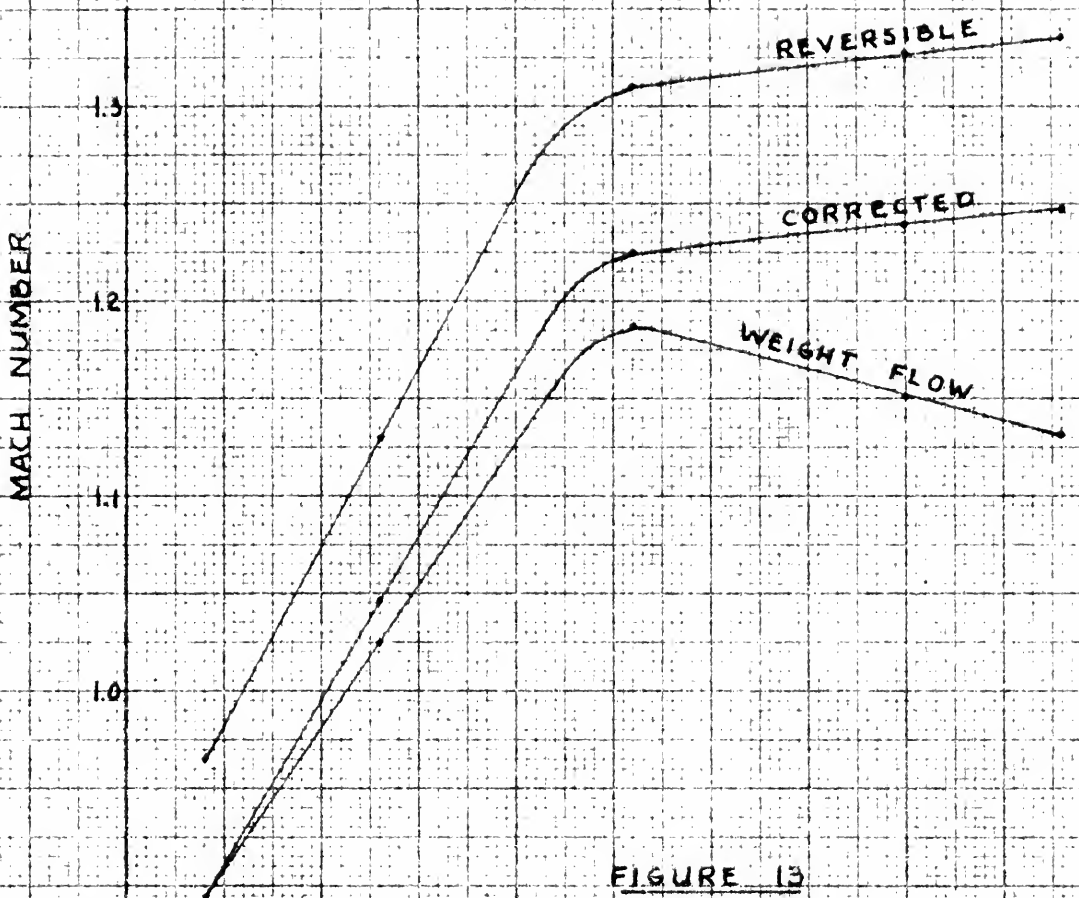

FIGURE 13

FRICTION FACTORS FOR RUNS OF SET 2

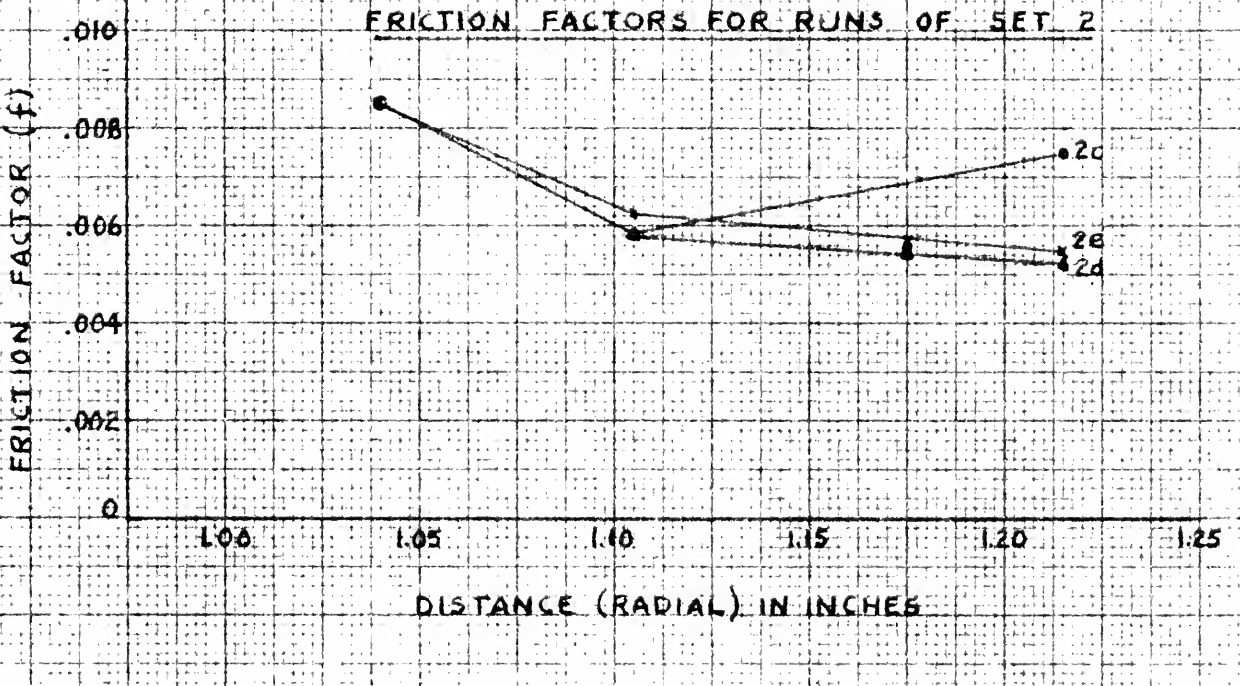

FIGURE 14

CURVES OF CORRECTED MACH NO. (M') VERSUS RADIAL DISTANCE FOR RUNS OF SET 2 WITH CONSTANT CLEARANCE (b)

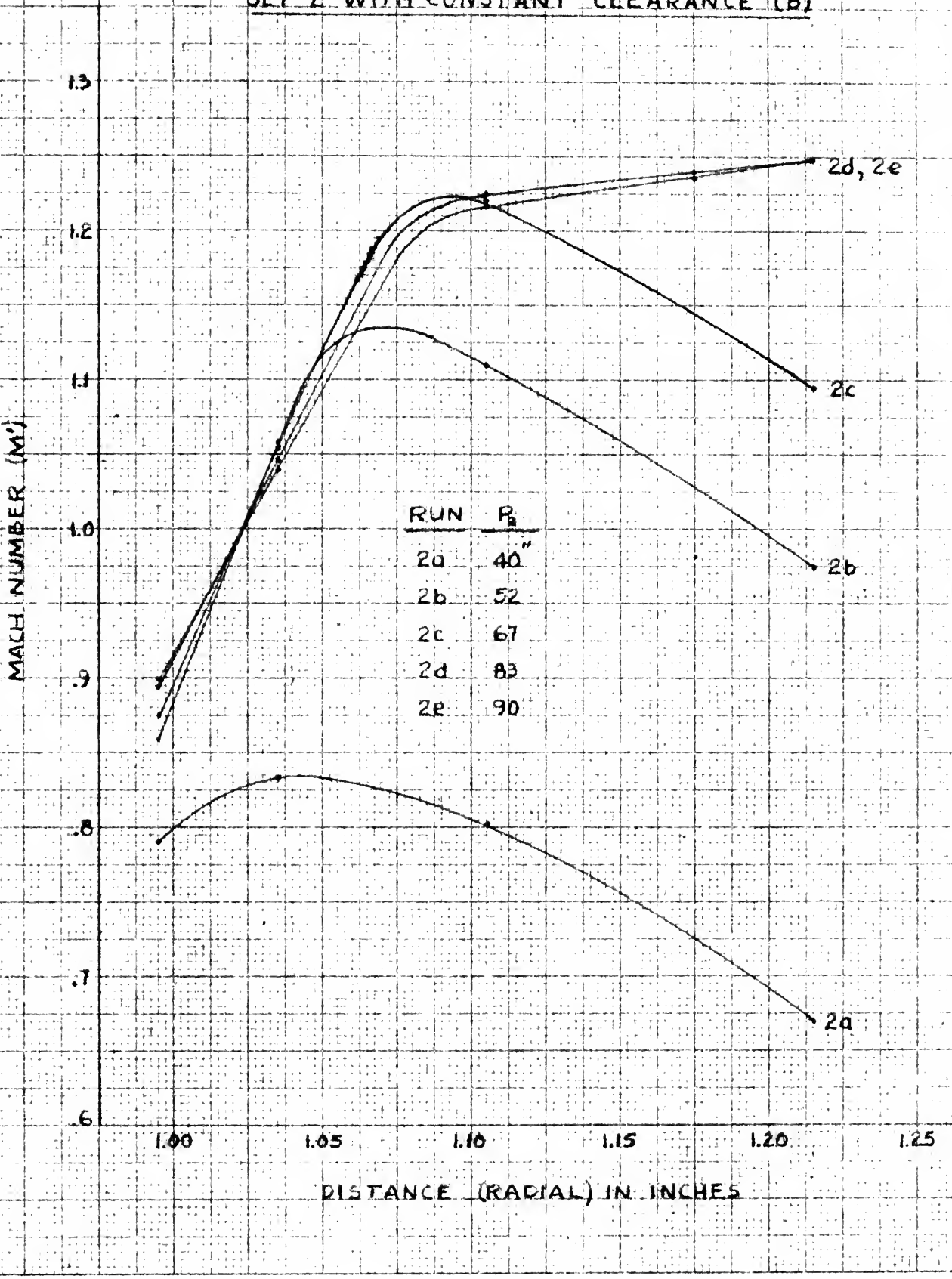

FIGURE 15

PROBABLE BOUNDARY LAYERS BASED ON CORRECTED FLOW AREAS FOR RUNS OF SET 2 (b = 0.036")

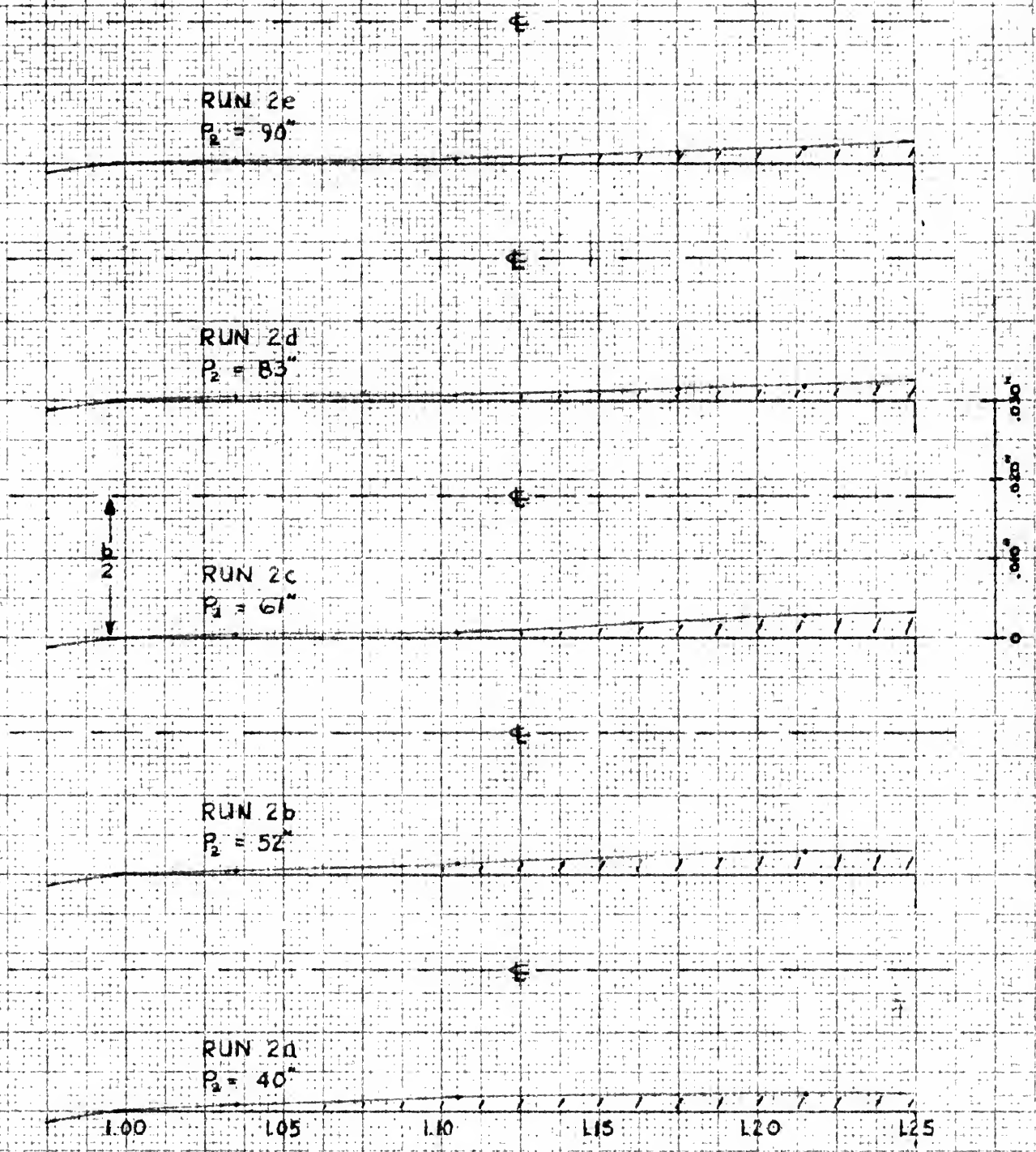

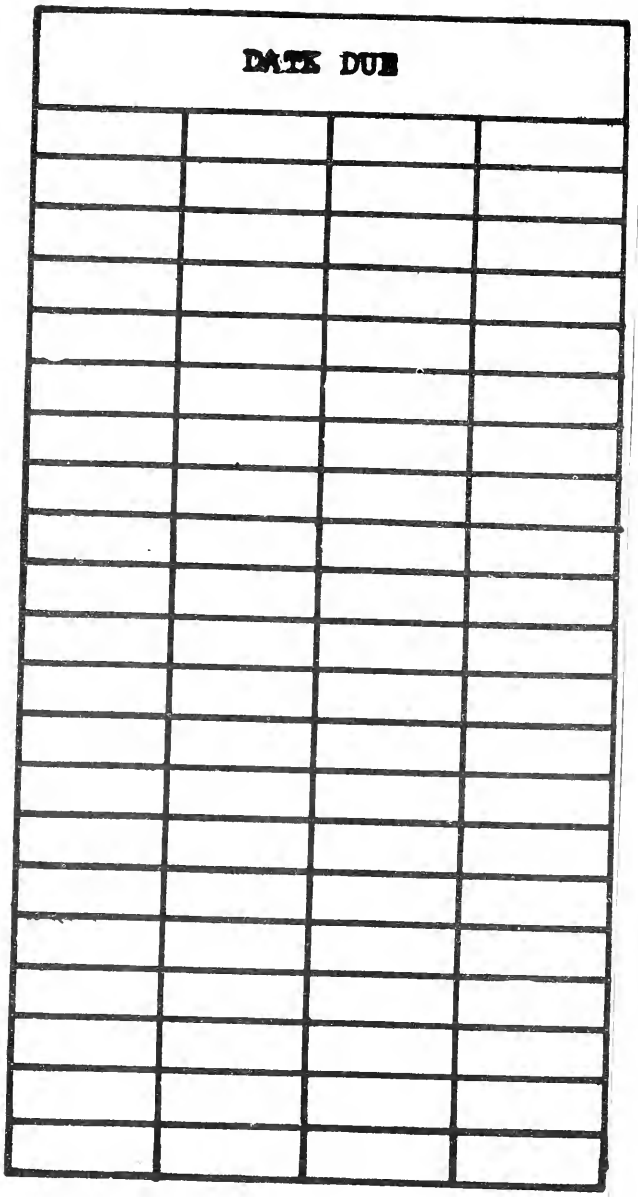
DATE DUE

Thesis 11257
G15 Gantar
An investigation of
high velocity radial
air flow.